Eur. Phys. J. C (2022) 82:873
https://doi.org/10.1140/epjc/s10052-022-10839-3

THE EUROPEAN PHYSICAL JOURNAL C

Regular Article - Theoretical Physics

Tests of standard cosmology in Hořava gravity, Bayesian evidence for a closed universe, and the Hubble tension

Nils A. Nilsson[1,a], **Mu-In Park**[2,b]

[1] National Centre for Nuclear Research, Pasteura 7, 00-293 Warsaw, Poland
[2] Center for Quantum Spacetime, Sogang University, Seoul 121-742, Korea

Received: 27 December 2021 / Accepted: 23 September 2022 / Published online: 5 October 2022

Abstract We consider some background tests of standard cosmology in the context of Hořava gravity with different scaling dimensions for space and time, which has been proposed as a renormalizable, higher-derivative, Lorentz-violating quantum gravity model without ghost problems. We obtain the "very strong" and "strong" Bayesian evidences for our two cosmology models **A** and **B**, respectively, depending on the choice of parametrization based on Hořava gravity, against the standard, spatially-flat, LCDM cosmology model based on general relativity. An MCMC analysis with the observational data, including BAO, shows (a) preference of a *closed* universe with the curvature density parameter $\Omega_k = -0.005 \pm 0.001$, $-0.004^{+0.003}_{-0.001}$, (b) reduction of the Hubble tension with the Hubble constant $H_0 = 71.4^{+1.2}_{-0.9}$, $69.5^{+1.6}_{-0.9}$ km s^{-1} Mpc^{-1} for the models **A**, **B**, respectively, and also (c) a positive result on the discordance problem. We comment on some possible further improvements for the "cosmic-tension problem" by considering the more complete early-universe physics, based on the Lorentz-violating standard model with anisotropic space-time scaling, consistently with Hořava gravity, as well as the observational data which are properly adopted for the closed universe.

Standard cosmology, which is usually formulated as the Lambda Cold Dark Matter (LCDM) model, is based on general relativity (GR) with a positive cosmological constant [1–3] and has been quite successful in describing the observational data [4]. However, with the increased accuracy of data, the significant deviations from LCDM are becoming clearer [5–7]. In particular, regarding the recent discrepancies of the Hubble constant from the Cosmic Microwave Background (CMB) data and the direct (local) measurements at the lower redshift, which corresponds to the mismatches between the early and late universes, there have been various proposals (for recent reviews, see [8–10]) but it is still a challenging problem to find a resolution at the fundamental level.

On the other hand, if our universe was created from the Big Bang, we need a *quantum gravity* to describe the early universe or later space-time. But, it has been well known that a renormalizable quantum gravity can not be realized in GR or its (relativistic) higher-derivative generalizations, due to the ghost problem [11]. Recently, Hořava has proposed a renormalizable, higher-derivative, *Lorentz-violating* quantum gravity model without the ghost problem, due to the high-energy (UV) Lorentz-symmetry violations from the different scaling dimensions for space and time *à la* Lifshitz, DeWitt, and Hořava [12–14]. In the last 12 years, there have been many works on its various aspects (see [15] for a review and extensive literatures). Theoretically, there are still several fundamental issues, like the full/complete symmetry structure, full dynamical degrees of freedom, renormalizability, and the very meaning of black holes and Hawking radiation, etc. (see [16] for related discussions and their current status). However, phenomenologically, Hořava gravity is one of the (viable) modified gravity theories and it can be tested from astrophysical or cosmological observations [17]. In particular, from the recent detections of gravitational waves from black holes/neutron stars, the importance of quantum gravity and its *non-GR* behaviors is increasing [18]. There are some interesting results on *testable* Hořava gravity effects, such as the increased maximum mass of neutron stars [19], reduced light deflection [20] and black hole shadow [21], etc. There are also some constraints on its low-energy limit

Nils A. Nilsson: On leave from *Rutherford Appleton Laboratory (RAL), Harwell Campus, Didcot, OX11 0QX, UK*.

[a] e-mail: albin.nilsson@ncbj.gov.pl
[b] e-mail: muinpark@gmail.com (corresponding author)

or Einstein-Aether theory from astrophysical data [22–25] or cosmological data with the "assumed" spatially-*flat* universe in standard cosmology [26,27]. But still, for a renormalizable Hořava gravity with the desired higher-derivative terms, there are no *systematic* and *significant* constraints from the observational data.

In this paper, we test the spatially *non-flat* universe in standard cosmology in the context of Hořava gravity. A peculiar property of the cosmology based on Hořava gravity is that the spatially-curved universe may be more "natural" due to contributions from higher spatial derivatives. For the spatially-flat universe, on the other hand, the usual FLRW *background* cosmology in Hořava gravity [1,2] is the same as in GR and hence there are no observable differences in the data analysis which means the same (background) tensions in LCDM model. In other words, Hořava gravity is a "natural laboratory" for the tests of the spatially non-flat universe in standard cosmology.

Recently, it has been found [28–31] that the tensions get worse in LCDM as $-\Omega_k$ increases, i.e, a rather lower value of Hubble constant for a closed universe ($\Omega_k < 0$), which is preferred in the recent Planck CMB data [32], without being combined with lensing and Baryon Acoustic Oscillations (BAO). In this paper, we show that the situation in Hořava gravity is the opposite, i.e., tensions get better with an increasing $-\Omega_k$, due to some non-linear corrections from (spatial) higher-derivative terms. From an MCMC analysis with the observational data, including BAO, we obtain (a) preference of a *closed* universe and (b) reduction of the Hubble tension for our two Hořava-gravity based cosmological models **A** and **B**, depending on the choice of parametrization, with "very strong" and "strong" Bayesian evidences, respectively, against the standard, spatially-flat, LCDM cosmological model.

To this ends, we consider the ADM (Arnowitt–Deser–Misner [33]) metric

$$ds^2 = -N^2c^2dt^2 + g_{ij}\left(dx^i + N^i dt\right) \times \left(dx^j + N^j dt\right) \tag{1}$$

and the Hořava gravity action with $z = 3$, *à la* Lifshitz, DeWitt, and Hořava [12–14], given by (up to boundary terms)

$$S_g = \int dtd^3x\sqrt{g}N\left[\frac{2}{\kappa^2}\left(K_{ij}K^{ij} - \lambda K^2\right) - \mathcal{V}\right], \tag{2}$$

$$-\mathcal{V} = \sigma + \xi R + \alpha_1 R^2 + \alpha_2 R_{ij}R^{ij} + \alpha_3\frac{\epsilon^{ijk}}{\sqrt{g}}R_{il}\nabla_j R^l{}_k + \alpha_4\nabla_i R_{jk}\nabla^i R^{jk} + \alpha_5\nabla_i R_{jk}\nabla^j R^{ik} + \alpha_6\nabla_i R\nabla^i R, \tag{3}$$

which is viable[1] [36] and power-counting renormalizable [37], with the extrinsic curvature

$$K_{ij} = \frac{1}{2N}\left(\dot{g_{ij}} - \nabla_i N_j - \nabla_j N_i\right) \tag{4}$$

(the dot ($\dot{}$) denotes a time derivative), the Ricci tensor R_{ij} of the (Euclidean) three-geometry, their corresponding traces $K = g_{ij}K^{ij}$, $R = g_{ij}R^{ij}$, coupling constants[2] $\kappa, \lambda, \xi, \alpha_i$, and a cosmological constant parameter σ.

In order to study standard cosmology for the Hořava gravity action (2), we consider the homogeneous and isotropic Friedmann–Lemaitre–Robertson–Walker (FLRW) metric ansatz

$$ds^2 = -c^2dt^2 + a^2(t) \times \left[\frac{dr^2}{1 - kr^2/R_0^2} + r^2\left(d\theta^2 + \sin^2\theta d\phi^2\right)\right] \tag{5}$$

with the (spatial) curvature parameter $k = +1, 0, -1$ for a closed, flat, open universe, respectively, and the curvature radius R_0 in the current epoch $a(t_0) \equiv 1$. Assuming the perfect fluid form of matter contributions with energy density ρ and pressure p, we obtain the Friedmann equations as

$$H^2 = \frac{\kappa^2}{6(3\lambda - 1)}\left[\rho + \frac{3\kappa^2\mu^2}{8(3\lambda - 1)} \times \left(\frac{k^2}{R_0^4a^4} + \frac{2k(\omega - \Lambda_W)}{R_0^2a^2} + \Lambda_W^2\right)\right], \tag{6}$$

$$\dot{H} + H^2 = \frac{\ddot{a}}{a} = \frac{-\kappa^2}{6(3\lambda - 1)} \times \left[\frac{1}{2}(\rho + 3p) + \frac{3\kappa^2\mu^2}{8(3\lambda - 1)}\left(\frac{k^2}{R_0^4a^4} - \Lambda_W^2\right)\right], \tag{7}$$

where we have used the conventional parametrization of the coupling constants $\sigma, \xi, \alpha_1, \alpha_2$ for the lower-derivative terms

[1] At the perturbation level, even for the spatially-flat background, Hořava gravity produces notable differences from GR. In order to obtain a (nearly) scale-invariant CMB power spectrum for the spatially-flat universe in Hořava gravity, where the "inflation without inflation era" is possible [34,35], we need a *proper* form of the six-derivative (UV) terms which break the detailed balance condition in UV as in the action (2) [36]. It would be interesting to see the curvature-induced effect on the scale-invariant power spectrum. However, in this paper, we consider the action (2) without any UV conditions for the generality of our approach.

[2] One might consider extension terms which depend on $a_i = \partial_i N/N$ and $\nabla_j a_i$ generally [38]. However, since these terms considerably affect the IR physics compared to those in the standard action (2) [39,40], we do not consider those terms in this paper by assuming that the IR physics is well described by GR. This implies that the gravity probe E_G approaches the GR prediction in the current epoch, i.e., low z, though currently it would not be tested due to large statistical errors [41].

[14,42,43]

$$\sigma = \frac{3\kappa^2\mu^2\Lambda_W^2}{8(3\lambda-1)},\ \xi = \frac{\kappa^2\mu^2(\omega-\Lambda_W)}{8(3\lambda-1)},$$
$$\alpha_1 = \frac{\kappa^2\mu^2(4\lambda-1)}{32(3\lambda-1)},\ \alpha_2 = -\frac{\kappa^2\mu^2}{8} \tag{8}$$

with an IR-modification parameter ω [42,43], $\mu^2 > 0$ (< 0) for a positive (negative) cosmological constant ($\sim \Lambda_W$), and the Hubble parameter $H(t) \equiv \dot{a}/a$. However, we take the coupling constants $\alpha_3, \ldots, \alpha_6$ for higher-derivative (UV) terms to be arbitrary so that a (nearly) scale-invariant CMB spectrum with respect to the background universe, as well as power-counting renormalizability, can be obtained [36].[3] However, it is important to note that there are no contributions in the above Friedmann equations from the fifth and sixth-derivative UV terms in the Hořava gravity action (2) due to $R_{ij} = 2kg_{ij}/R_0^2a^2(t)$, $K_{ij} = H(t)g_{ij}$, but only from the fourth-derivative terms, which leads to k^2/a^4 terms[4] in the Friedmann equations (6) and (7). On the other hand, for the spatially-flat universe with $k = 0$, all the contributions from the higher-derivative terms disappear and we recover the same background cosmology as in GR, which means a return to the LCDM model with the Hubble constant tension. In this sense, Hořava gravity is a "natural laboratory" for the tests of the spatially non-flat universe in standard cosmology.

Introducing dust matter (non-relativistic baryonic matter and (non-baryonic) cold dark matter with $p_m = 0$) and radiation (ultra-relativistic matter with $p_r = \rho_r/3$), which satisfy the continuity equations $\dot{\rho}_i + 3H(\rho_i + p_i) = 0$ $(i = m, r)$, we conveniently define the canonical density parameters at the current epoch $a_0 = 1$ as[5]

$$\Omega_m \equiv \beta\frac{\rho_m^0}{3H_0^2},\ \Omega_r \equiv \beta\frac{\rho_r^0}{3H_0^2},\ \Omega_k \equiv -\gamma\frac{k}{H_0^2R_0^2},$$
$$\Omega_\Lambda \equiv \gamma\frac{\Lambda_W}{2H_0^2},\ \Omega_\omega \equiv \gamma\frac{\omega}{2H_0^2}, \tag{9}$$

where $\beta \equiv \kappa^2/2(3\lambda-1)$, $\gamma \equiv \kappa^4\mu^2\Lambda_W/8(3\lambda-1)^2$ are positive constant parameters. Then, we can write the (first) Friedmann equation (6) as

$$\left(\frac{H}{H_0}\right)^2 = \Omega_r a^{-4} + \Omega_m a^{-3} + \Omega_k a^{-2} + \Omega_{\rm DE}(a), \tag{10}$$

where we have introduced the (dynamical) dark-energy (DE) component as

$$\Omega_{\rm DE}(a) \equiv \left(\frac{\Omega_k^2}{4\Omega_\Lambda}\right)a^{-4} - \left(\frac{\Omega_k\Omega_\omega}{\Omega_\Lambda}\right)a^{-2} + \Omega_\Lambda, \tag{11}$$

which is defined as all the extra contributions to the first-three GR terms in (10) [42,43]. Here, we note that this dynamical dark-energy component includes the *dark radiation* (DR) and *dark curvature* (DC) components as

$$\Omega_{\rm DR}(a) \equiv \left(\frac{\Omega_k^2}{4\Omega_\Lambda}\right)a^{-4},\ \Omega_{\rm DC}(a) \equiv -\left(\frac{\Omega_k\Omega_\omega}{\Omega_\Lambda}\right)a^{-2}, \tag{12}$$

which play the roles of the extra radiation and curvature terms, respectively, as well as the usual cosmological constant component Ω_Λ, so that $\Omega_{\rm DE}(a) = \Omega_{\rm DR}(a) + \Omega_{\rm DC}(a) + \Omega_\Lambda$.

So far we have not assumed any specific information about the early universe. The whole physics of early universe in the context of Hořava gravity would be quite different from our known physics and needs to be revisited for a complete analysis. However, as in the standard cosmology, we may introduce the phenomenological parametrization so that all the unknown (early-universe) physics can be taken into account. For example, regarding the Big Bang Nucleosynthesis (BBN) at the decoupling epoch $a_{\rm dec} = (1+z_{\rm dec})^{-1} = (1091)^{-1}$, the *early dark radiation* can be expressed as the contribution from the hypothetical excess $\Delta N_{\rm eff}$ in the standard model prediction of the effective number of relativistic species $N_{\rm eff} = 3.046$ as [46]

$$\Omega_{\rm DR}(a) \equiv \frac{7}{8}\left(\frac{4}{11}\right)^{4/3}\Delta N_{\rm eff}\,\Omega_\gamma a^{-4}$$
$$= 0.13424\,\Delta N_{\rm eff}\,\Omega_r a^{-4}, \tag{13}$$

where we have used the present radiation density parameter for the standard model particles with negligible masses (photon and three species of neutrinos), $\Omega_r = [1 + \frac{7}{8}(\frac{4}{11})^{4/3}N_{\rm eff}]\,\Omega_\gamma = \frac{7}{8}(\frac{4}{11})^{4/3}\cdot(0.13424)^{-1}\Omega_\gamma$ with the photon density $\Omega_\gamma = 2.4730\times10^{-5}h^{-2}$ for the present CMB temperature $T_0 = 2.7255\,{\rm K}$ [32] and $h \equiv H_0/100\,{\rm km\,s^{-1}\,Mpc^{-1}}$. If we use the relation (13) for the dark radiation formula (12) in Hořava gravity, we can express the cosmological constant component Ω_Λ as

$$\Omega_\Lambda = \frac{\Omega_k^2}{4\cdot0.13424\,\Delta N_{\rm eff}\,\Omega_r} \tag{14}$$

so that the Friedmann equation (10) can be written by $\Delta N_{\rm eff}$, instead of Ω_Λ [44,47]. Here, it is important to note that $\Delta N_{\rm eff}$ needs not to be an integer but can be an arbitrary and positive (negative) real number for a positive (negative) Ω_Λ, i.e., asymptotically *de Sitter* (*Anti de Sitter*) universe with a cosmological constant $\sim \Lambda_W$. Moreover, we note that

[3] For the cosmological perturbation around the spatially-flat FLRW background, the scale-invariant spectrum for the tensor modes depend only on the coupling α_4, whereas the scalar mode depends on the combination $\widetilde{\alpha}_4 \equiv \alpha_4 + 2\alpha_5/3 + 8\alpha_6/3$.

[4] If we include *non-derivative* higher-curvature terms, like R^3, $R^2R_{ij}R^{ij}$, etc., we have a^{-6} terms as well, which correspond to *stiff* matter [44,45]. However, in this paper we do not consider those terms for simplicity.

[5] We adopt the common convention Ω_i for the current values and $\Omega_i(a)$ for the fully time-dependent values.

Table 1 Constraints at 1σ (68%) CL errors on the cosmological parameters for our two cosmology models **A**, **B**, based on Hořava gravity, and the standard cosmology models, spatially-flat ($k = 0$) LCDM and spatially-non-flat ($k \neq 0$) kLCDM, based on GR. In the bottom lines, we show $\chi^2_{\rm min}$ for the best-fit values of parameters, the (logarithmic) Bayesian evidence $\ln E$, and the Bayes factor $\ln B_{ij}$ with respects to LCDM. $\Delta\chi^2_{\rm min}$ represents the difference of $\chi^2_{\rm min}$ from those of LCDM. The **bold-faced** quantities represent the derived quantities

Model Parameters	Model **A**	Model **B**	kLCDM	LCDM
$\Omega_b h^2$	0.0227 ± 0.0001	0.0227 ± 0.0001	0.0226 ± 0.0001	0.0225 ± 0.0001
Ω_m	$\mathbf{0.307 \pm 0.004}$	$\mathbf{0.306^{+0.005}_{-0.006}}$	$\mathbf{0.302 \pm 0.005}$	$\mathbf{0.305 \pm 0.004}$
$\Omega_r \cdot 10^5$	$\mathbf{8.20^{+0.22}_{-0.27}}$	$\mathbf{8.64^{+0.23}_{-0.38}}$	$\mathbf{8.93^{+0.14}_{-0.13}}$	$\mathbf{8.94^{+0.08}_{-0.08}}$
Ω_k	-0.005 ± 0.001	$-0.004^{+0.003}_{-0.001}$	-0.001 ± 0.002	–
Ω_Λ	$\mathbf{0.70 \pm 0.01}$	0.695 ± 0.005	0.699 ± 0.004	0.695 ± 0.004
H_0 [km s^{-1} Mpc^{-1}]	$71.38^{+1.19}_{-0.93}$	$69.53^{+1.57}_{-0.91}$	$68.41^{+0.52}_{-0.51}$	$68.36^{+0.32}_{-0.30}$
Ω_ω	$-0.75^{+0.46}_{-0.24}$	$0.34^{+1.15}_{-0.31}$	–	–
$\Delta N_{\rm eff}$	$0.87^{+0.28}_{-0.26}$	–	–	–
$\chi^2_{\rm min}$	1143.6	1150.1	1155.0	1157.9
$\Delta\chi^2_{\rm min}$	−14.3	−7.8	−2.9	0
$\ln E$	−573.8	−576.9	−578.9	−580.0
$\ln B_{ij}$	+6.2	+3.1	+1.1	0

the relation (14) implies an intriguing correlation between Ω_k, Ω_r, $\Delta N_{\rm eff}$, and Ω_Λ, which are otherwise unrelated.

In this paper, we consider two models, **A** and **B**, depending on whether we implement (14) or not, to see the effectiveness of the BBN-like parametrization in terms of $\Delta N_{\rm eff}$. Then, for model **A**, the Friedmann equation (10) reduces to

$$\left(\frac{H}{H_0}\right)^2 = (1 + 0.13424\ \Delta N_{\rm eff})\Omega_r a^{-4} + \Omega_m a^{-3} + \left[\Omega_k - 4 \cdot 0.13424\ \Delta N_{\rm eff}\left(\frac{\Omega_\omega \Omega_r}{\Omega_k}\right)\right] a^{-2} + \frac{\Omega_k^2}{4 \cdot 0.13424\ \Delta N_{\rm eff}\ \Omega_r}, \tag{15}$$

which is one of our main equations for comparing with cosmological data, with the assumption of non-vanishing Ω_k and $\Delta N_{\rm eff}$ for the well-defined equation (15). Here we note that, considering Ω_r is a function of H_0 as given above, this model is described by five non-linearly coupled parameters $H_0, \Omega_m, \Omega_k, \Omega_\omega, \Delta N_{\rm eff}$, in contrast to the three linear, decoupled parameters $H_0, \Omega_m, \Omega_\Lambda$ for the standard, spatially-flat (background) cosmology, LCDM.[6]

On the other hand, for model **B**, the Friedmann equation (10) is simply given by

$$\left(\frac{H}{H_0}\right)^2 = \left(\Omega_r + \frac{\Omega_k^2}{4\Omega_\Lambda}\right) a^{-4} + \Omega_m a^{-3} + \left(1 - \frac{\Omega_\omega}{\Omega_\Lambda}\right)\Omega_k a^{-2} + \Omega_\Lambda \tag{16}$$

without using the relation (14) from the BBN-inspired formula (13) for the dark radiation in Hořava gravity. This model has two (non-linearly) coupled parameters Ω_k and Ω_ω, in addition to those of standard flat cosmology, H_0, Ω_Λ, with assuming a non-vanishing Ω_Λ for the well-defined equation (16). We also consider the spatially flat ($k = 0$) LCDM as well as non-flat ($k \neq 0$) kLCDM for comparison.

We probe our universe by using a Markov-Chain Monte Carlo (MCMC) method for the four models, **A**, **B**, LCDM, kLCDM and determine the independent parameters with the statistical inferences for the models. We use the Metropolis–Hastings algorithm[7] [48] for the posterior parameter distributions, the statistical method in [49] for convergence tests of the MCMC chains, and the public code GetDist [50] for the visualization of the results. The cosmological data sets we consider (for the details, see Appendix A) are CMB (Planck 2018 [51]), BAO (SDSS-BOSS [52], SDSS-IV [53], Lyman-α forest [54], and WiggleZ [55]), SNe Ia (Pantheon [56]),

[6] From the current-epoch constraint, i.e., $H(t_0) \equiv H_0$ in (10), the number of independent parameters reduces to 4 and 2 for our two models based Hořava gravity and the standard models based on GR, respectively. In this paper, we conveniently take $H_0, \Omega_k, \Omega_\omega, \Delta N_{\rm eff}$ (or Ω_Λ) and $H_0, \Omega_k, \Omega_\Lambda$ for the models **A**, **B**, and (k)LCDM, respectively, by considering Ω_m, as well as Ω_r, as the derived (dependent) parameter. However, we need to introduce the baryonic parameter Ω_b as an independent parameter when we analyze CMB and BAO data later so that only the (non-baryonic) dark matter sector in Ω_m is the derived parameter.

[7] We use the Metropolis–Hastings algorithm at the background level since there is no known analysis of the cosmological perturbations for a non-flat universe, contrary to the flat universe [36], due to computational complications in Hořava gravity. However, the algorithm has the limitation in our case, though not a general feature, that does not show the proper χ^2 values for the *separate* data sets, while it shows the convergent results for the *whole* data sets.

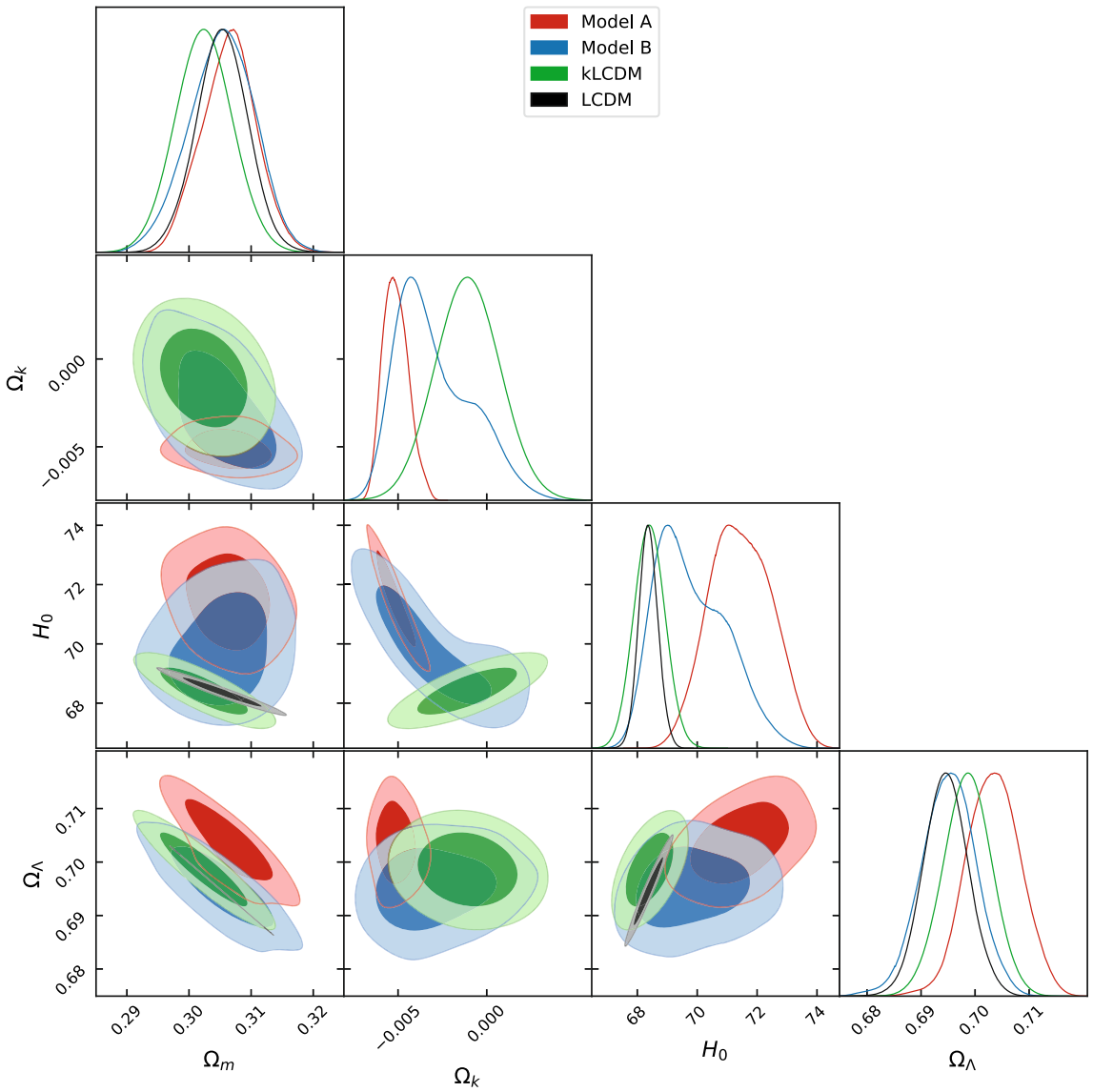

Fig. 1 2D joint and 1D marginalized posterior probability distributions for Ω_m, Ω_k, H_0, and Ω_Λ, obtained within our two models **A**, **B** and the standard cosmology models, spatially-flat LCDM, spatially-non-flat kLCDM. Contour plots are shown at 1σ (68%) and 2σ (95%) CL

GRBs (Mayflower [57]), Lensed Quasars (H0liCOW [58]), and Cosmic Chronometers (CC) [59]. Here, it is important that we need to include CMB lensing data in combination with BAO or SNe Ia in order to test the curvature of the universe [60,61].

Our main results are shown in Table 1 and their essentials are plotted in Fig. 1 (for the full plots, see Appendix B). Some noticeable results are as follows:

1. For our two main models **A** and **B**, constraints with all the data sets, including BAO, show some reduced tensions in the Hubble constant H_0, from the direct local measurements using Cepheids [5] (see Fig. 2 for a comparison with other previous measurements [62–66]). In particular, for model **A**, the tension is reduced to within 1σ even if BAO data is included.

On the other hand, for Ω_m and Ω_Λ, there are only some slight differences from the standard LCDM or kLCDM, and the conventional constraint of $\Omega_m \approx 0.3$ and $\Omega_\Lambda \approx 0.7$ [3] is still robust even in Hořava cosmology. This result is important because it may indicate a resolution of the *discordance* problem in the LCDM paradigm, which constrains $\Omega_m \sim 0.5$, $\Omega_\Lambda \sim 0.5$ when a *closed* universe is considered as preferred by Planck [28,29], but *incompatible* with other local measurements. However, since our result may not be its complete confirmation because we do not have the results for separate data sets but only for their combinations, as noted in the footnote No. 7.

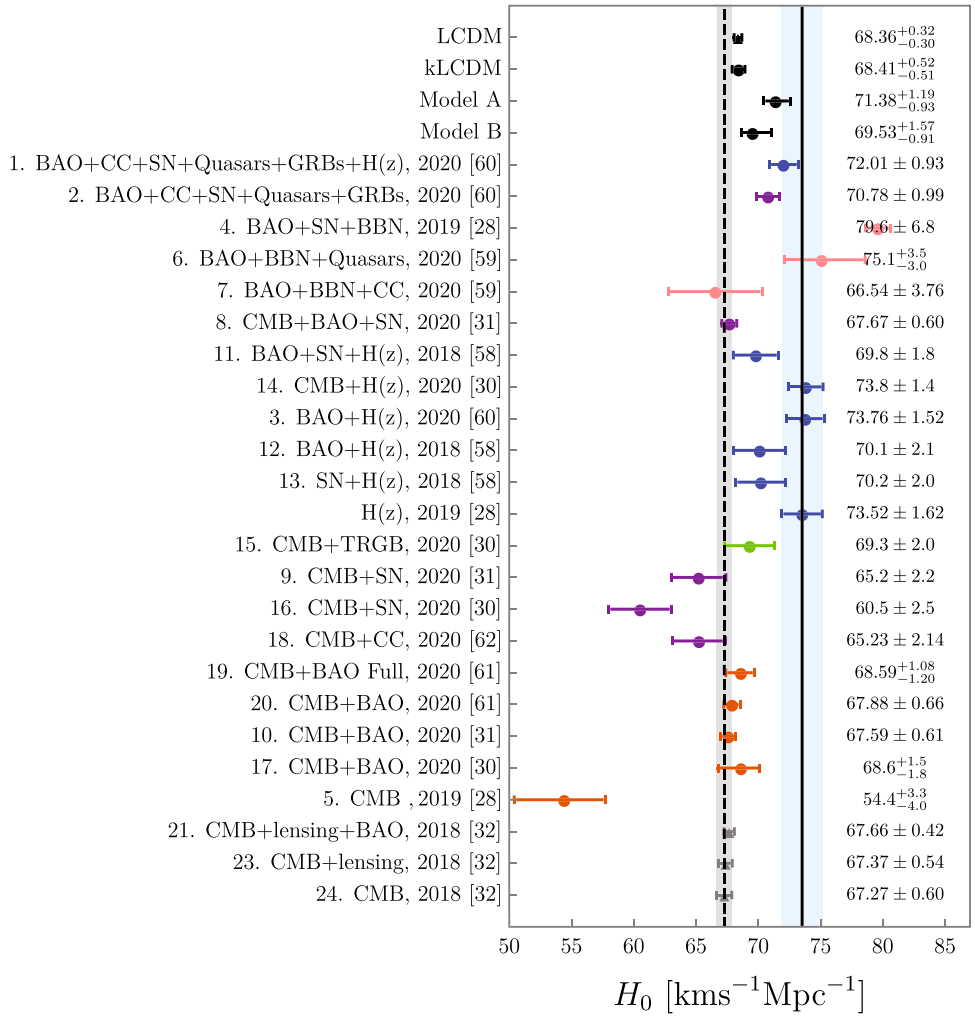

Fig. 2 Constraints on the Hubble constant H_0 at 1σ CL obtained by different measurements vs. our constraints for the models **A**, **B**, LCDM, and kLCDM, using all the data sets in Table 1. In the different measurements, we use all the *non-flat* universe analysis (their companions with the same left numbers in Fig. 3) except the $H(z)$ data [28] and the bottom three data [32], and the full analysis (without priors) for all the CMB data, in contrast to our analysis with the CMB priors. The grey vertical band corresponds the value $H_0 = 67.27 \pm 0.60$ km s^{-1} Mpc^{-1} as reported by Planck 2018 team [32] within a LCDM scenario. The blue vertical band corresponds to the value $H_0 = 73.52 \pm 1.62$ km s^{-1} Mpc^{-1} from the recent direct local measurement using Cepheids [6]

The constraint of Ω_r, for model **A**, is not overlapping within 2σ CL of the Planck 2018 data, $(9.179^{+0.441}_{-0.431}) \times 10^{-5}$ (CMB+lensing+BAO) [67]. However, it is not surprising that Ω_r, which is a derived quantity from the standard formula below Eq. (13) and reduced by a factor H_0^{-2} from the increased constraint on H_0, which is in about 4σ tension with the Planck 2018 data $H_0 = 67.27 \pm 0.60$ km s^{-1} Mpc^{-1} [32], has a similar tension with the Planck data.

The constraints of Ω_ω are rather different for models **A** and **B**. Ω_ω is a newly introduced parameter in our models and it has no a priori known constraint. But our results show that $\Omega_\omega < 0$ is preferred at 1.6σ for model **A** so that $\Omega_k \Omega_\omega > 0$, whilst poorly constrained for model **B**.

2. Ω_k is peculiar in two aspects as follows. First, the result for model **A** shows a higher precision, i.e., narrower MCMC contour (see Ω_k vs. Ω_m in Fig. 1, for example) and, as a result, a closed universe, i.e., $\Omega_k < 0$, is more strongly preferred than in kLCDM (cf. [8]). (See Fig. 3 for the comparisons with other results based on a minimal extension to LCDM) This is peculiar because the lower precision (i.e., wider distribution) is normally expected with the addition of more parameters, as can be seen in $\Omega_b h^2$, Ω_r, and H_0 for **A** and **B**, in contrast to kLCDM. Second, the correlation between H_0 and Ω_k is quite different for **A** or **B** and kLCDM: As $-\Omega_k$ increases, i.e., the universe tends more towards a closed universe, H_0 increases for **A** and **B**, i.e., the two parameters are *anti-correlated*, whereas the situation is the opposite for kLCDM. This property for H_0 resolves the problem of Hubble constant tension in kLCDM [28,30][8] (see Fig. 5 for the H_0 vs. Ω_k tension in the measurements of Figs. 2 and 3). These peculiar properties seem to be due to the non-linear coupling of Ω_k in the Friedmann equations (15) and (16).

3. In our analysis, we use the CMB distance priors, or shift parameters, instead of the full CMB data (for the details, see Appendix A). It is possible that this choice may lead to a lower statistical weight generally, though it has been widely used and is a convenient substitute of the full CMB data. However, the comparison of our analysis for the kLCDM or LCDM case and the full CMB analysis in Fig. 2 when com-

[8] It is interesting that a similar effect of curvature has been noted earlier in [6] (see Fig. 4) though it would be hardly justified in the data sets with the CMB, based on GR [65,66].

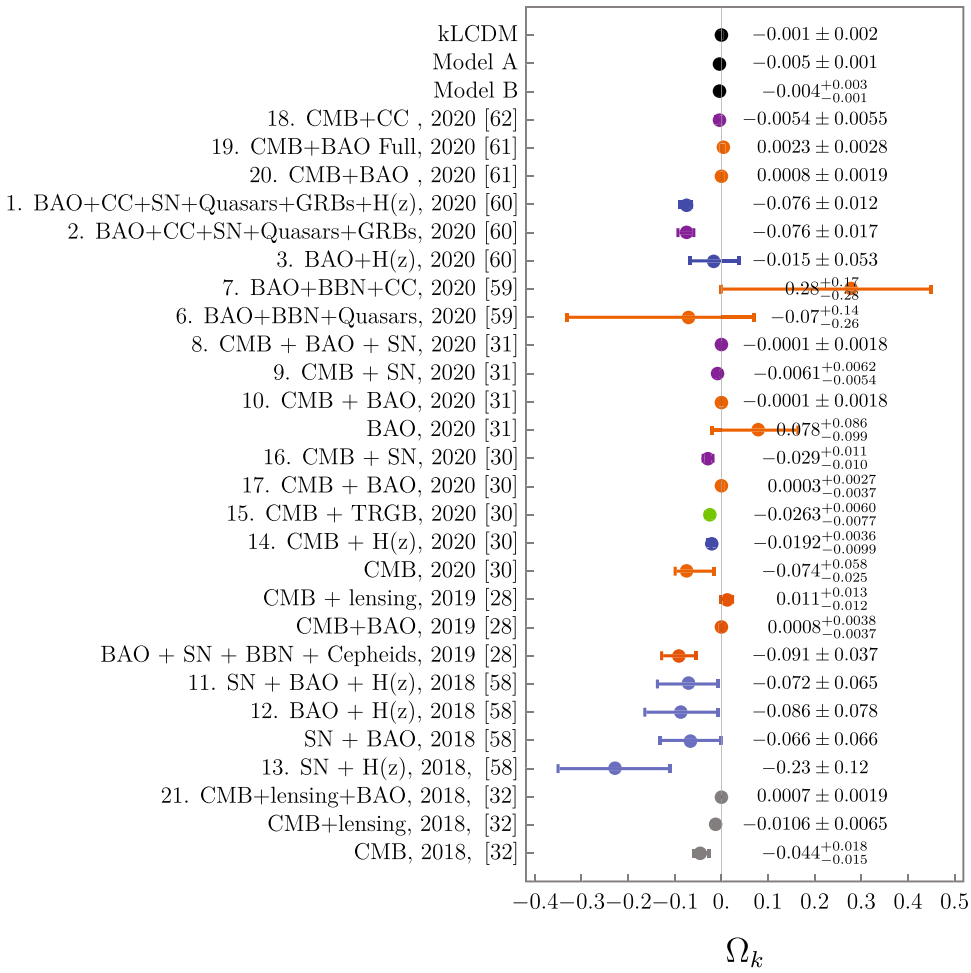

Fig. 3 Constraints on Ω_k at 1σ CL obtained by different measurements based on a minimal extension to LCDM vs. our constraints for the models **A**, **B**, and kLCDM, with all the data sets in Table 1. The corresponding companions in Fig. 2 have the same left numbers

bining other data sets, including BAO, shows that it has just a small effect as can be seen. For example, CMB+BAO+SN [31], CMB+BAO Full [65], CMB+lensing+BAO [32] (with or without Ω_k) that use the full CMB data, show a few percent effects ($< 2\%$), in comparison with our LCDM, kLCDM results with the CMB priors.[9]

4. The constraint of $\Delta N_{\rm eff}$, for model **A** (considering its central value), is *consistent* with SPT-3G 2018 data (alone), 0.65 ± 0.70 (CMB)[10] [69] by 0.31σ, while in a *tension* with Planck 2018 data, for example, 2.7–2.8 σ of $-0.06^{+0.34}_{-0.33}$ (CMB+lensing+BAO) [32]. Since, in our MCMC analysis, we have not included SPT-3G 2018 data, which gives better constraints at the higher angular multipoles $l > 1000$, the agreement of our constraint of $\Delta N_{\rm eff}$ might give an independent support of our model **A**. However, due to the lack of data with both $\Delta N_{\rm eff}$ and Ω_k, which would be quite (anti-)correlated (see Fig. 4), as the *varying* parameters in SPT and Planck, the exact quantification of (in)compatibility is not available yet. But we can generally expect some tensions with Planck 2018 in $\Delta N_{\rm eff}$ as in the case of H_0, due to the correlation of $\Delta N_{\rm eff}$ and H_0 in Planck 2018 [32,69], as well as in SPT-3G 2018 [69] and our case (Fig. 4).

It is known that primordial gravitational waves may add to the effective relativistic degrees of freedom [70]. For example, in a recently proposed scenario linking $\Delta N_{\rm eff}$ with the gravitational waves from primordial black holes [71], it is possible to have $\Delta N_{\rm eff\,(GW)} \sim 0.1$–$0.2$ which may increase the standard value $N_{\rm eff} = 3.046$ and its associated radiation parameter Ω_r, slightly. In some different scenarios, it has been also found that the primordial gravitational waves do not solve but alleviate the H_0-tension problem [72]. However, in all those cases, a spatially-*flat* universe is assumed *implicitly* and the effect of a non-flat universe seems to still be an open problem. Moreover, due to some inaccuracies of the (as adopted by us) CMB priors for the primordial power spectrum in a non-flat universe [68], in this paper, we will not quantify its effect in the H_0-tension problem further which needs another full data analysis as well.

5. From Bayes theorem, the Bayesian evidence $E(\mathcal{D}|\mathcal{M})$ for a model $\mathcal{M}$ with the total data sets $\mathcal{D}$ is given by the

[9] There is a more systematic analysis on the test of the CMB priors which supports the use of the CMB priors for the background analysis of dark-energy dynamics [68]. It would be an interesting problem to confirm the accuracy of the CMB priors for our Hořava cosmology model also in a more systematic way.

[10] In this case, the constraint of H_0 is given by 73.5 ± 5.2 km s^{-1} Mpc^{-1}.

integration over the model parameters θ

$$E(\mathcal{D}|\mathcal{M}) = \int d\theta\ \mathcal{L}(\mathcal{D}|\theta, \mathcal{M})\ \pi(\theta|\mathcal{M}), \tag{17}$$

where $\mathcal{L}(\mathcal{D}|\theta, \mathcal{M})$ is the likelihood $\mathcal{L}(\mathcal{D}|\theta, \mathcal{M}) \equiv exp[-\chi^2(\mathcal{D}|\theta, \mathcal{M})/2]$ in which the total χ^2 is obtained by summing $\chi^2(\mathcal{D}_i|\theta, \mathcal{M})$ over all the data sets $\mathcal{D}_i$. $\pi(\theta|\mathcal{M})$ is the prior probability, which we have assumed to be flat, i.e., no prior information on θ, in order to be as agnostic as possible: our only priors[11] are $0 < \Omega_b < \Omega_m$, $0 < H_0 < 100$ for LCDM, kLCDM; in addition, $\Omega_k \neq 0$, $\Delta N_{\rm eff} \neq 0$ for model **A** and $\Omega_\Lambda \neq 0$ for model **B**, in order to avoid the singularity of the corresponding Friedmann equations (15) and (16), respectively.[12] The differences of $\chi^2_{\rm min}$ for the models **A** and **B**, with respect to LCDM, $\Delta\chi^2_{\rm min} = -14.3, -7.8$ indicate the notable improvements of fitting to the given data sets, in contrast to the smaller difference $\Delta\chi^2_{\rm min} = -2.9$ for kLCDM.

For a more quantitative comparison of the models, we consider the Bayes factor

$$B_{ij} \equiv \frac{E(\mathcal{D}|\mathcal{M}_i)}{E(\mathcal{D}|\mathcal{M}_j)}, \tag{18}$$

which quantifies the preference for model $\mathcal{M}_i$ against model $\mathcal{M}_j$, using the (revised) Jeffrey's scale [73–75]: weak ($0 \leq \ln B_{ij} < 1.1$), definite ($1.1 \leq \ln B_{ij} < 3$), strong ($3 \leq \ln B_{ij} < 5$), very strong ($5 \leq \ln B_{ij}$). Table 1 gives the Bayes factors for model **A** and **B** with respect to LCDM, $\ln B_{ij} = +6.2, +3.1$, i.e., "very strong" and "strong" evidences, respectively, against the flat LCDM, in contrast to the "definite"[13] evidence for kLCDM with $\ln B_{ij} = +1.1$.[14]

6. The theory parameters can be written in terms of cosmological parameters as

$$\omega = -\frac{2k\Omega_\omega}{R_0^2\Omega_k},\ \Lambda_W = -\frac{2k\Omega_\Lambda}{R_0^2\Omega_k},\ \mu^2 = \left(\frac{\Omega_k}{-k}\right)\frac{H_0R_0M_P}{\Omega_\Lambda L_P}, \tag{19}$$

where M_P and L_P are the Planck mass and length, respectively, with $M_P/L_P = c^2/8\pi G = \alpha^{-1}$. Then we obtain their best-fit values,[15] $(\bar\omega,\ \bar\Lambda_W,\ \bar\mu) = (-275.94,\ 270.99,\ 0.0062)$, $(173.51,\ 390.24,\ 0.0043)$, where $\bar\omega \equiv \omega R_0$, $\bar\Lambda_W \equiv \Lambda_W R_0$, $\bar\mu \equiv \left(\mu^2 L_P/H_0R_0M_P\right)^{1/2}$, for the models **A** and **B**, respectively.[16] There are large errors (see Table 2 and Fig. 6) due to the non-linearity of the relation (19) but their best-fit values are distributed near what can be obtained by plugging in the obtained best-fit values of observational parameters in Table 1, $(\bar\omega,\ \bar\Lambda_W,\ \bar\mu) = (-299.20,\ 281.20,\ 0.00596)$, $(167.50,\ 347.50,\ 0.00479)$. These would be the first full (cosmological) determination of the theory parameters (for the earlier determinations,[17] see [42,43]).

In conclusion, we have tested the spatially non-flat universe in standard cosmology within Hořava gravity. We have obtained the "very strong" and "strong" Bayesian evidences against flat LCDM, for our two models **A** and **B**, respectively. Moreover, the MCMC analysis shows (a) the preference of a closed universe, (b) a reduction of the Hubble constant tension, and (c) a positive result on the discordance problem, even if BAO data is included. It is remarkable that just the use of (14) for model **A**, which gives a *novel* relation between $\Omega_\Lambda, \Omega_k, \Omega_r$ via $\Delta N_{\rm eff}$ which are otherwise unrelated, produces the difference in the results of the two models.

The reduced Hubble tension may be related to a natural inclusion of the (early) dark radiation within the dynamical dark energy and its associated contribution to $\Delta N_{\rm eff} = 0.87$ for model **A**, and the peculiar contribution of the curvature $\Omega_k < 0$, as have been previously considered on phenomenological ground [5,78]. However, the resolution does not seem to be quite complete yet [79]; this might be due to the fact that our observational data may not be completely model independent and are based on known physics. For example, as noted earlier, the BBN-like parametrization (13), which has been used for model **A**, is based on standard particle physics model with the phenomenological parameter $\Delta N_{\rm eff}$. Our MCMC analysis implies that the phenomenological approach of model **A** is a good approximation of the BBN, constraining Ω_k more precisely and reducing the Hubble constant tension, i.e., increasing H_0, with the almost doubled Bayesian evidence compared to model **B**. It would be a challenging problem to thoroughly consider the effect of anisotropic scaling beyond the standard model BBN and revisit the Hubble tension problem to see whether a com-

[11] In general, if the prior range is too small, the parameter chain can be seen to 'hit a wall' at one end of the prior (which serves as a hard cutoff), but we have not observed this behavior in our analysis. For the 2D contours in Fig. 4, in particular for Ω_k and Ω_w, we zoom out enough to show the details of model **A** as clearly as possible but at least without cutting out 2σ CL, in compatible with 2σ contours in Fig. 1. However, for the 1D contours of 1σ CL in Fig. 4, we have the desired vanishing tails of the posterior distributions at the boundary of the priors, and all of our results have passed the convergence tests in [49].

[12] The infinitesima widths of the excluded parameter regions, which are basically discrete, around the singularities are not fixed but randomly chosen in the MCMC analysis. But, the smooth contours around the singularities in Fig. 4 show that our chosen priors work well.

[13] This is in contrast to the "strong" evidence for kLCDM with $\ln B_{ij} = +3.3$ for CMB data alone [28].

[14] The detailed *decisiveness* of the results can depend on the adopted scales. For example, in Trotta's revisited scale [76], our results show "strong", "moderate", and"weak" evidence, respectively.

[15] It is interesting to note that this is the case of $\omega < 0$, $\omega < 2\Lambda_W$ in which the observer region is located between the inner and outer (black hole) horizons with the *cutting-edge* (surface-like) singularity of the space-time (or, the end of world) inside the inner horizon [77].

[16] These correspond to the CPL parameters, $(\omega_0,\ \omega_a) = (-1.005,\ -0.010)$, $(-0.998,\ 0.004)$ for the expansion of $\omega_{\rm DE} = \omega_0 + \omega_a(1-a) + \omega_b(1-a)^2 + \cdots$, near the current epoch $a = 1$.

[17] There are sign errors for the results of $\bar\omega$ and k in [42,43].

plete resolution can be found or not. Finally, the analysis of the cosmological perturbations for the non-flat universe and with the full use of Boltzmann solvers such as CAMB/Class [80,81] would also be an important arena for studying standard cosmology, like the cosmic-shear or σ_8 tension [28].

Acknowledgements We would like to thank Wayne Hu, Hyung-Won Lee, Seokcheon Lee, Seshadri Nadathur, Chan-Gyung Park, Vincenzo Salzano, and Eleonora Di Valentino for helpful discussions. We also thank to an anonymous referee for helpful comments which have inspired us to improve our paper. NAN and MIP were supported by Basic Science Research Program through the National Research Foundation of Korea (NRF) funded by the Ministry of Education, Science and Technology (2020R1A2C1010372) [NAN], (2020R1A2C1010372, 2020R1A6A1A03047877) [MIP].

Data Availability Statement This manuscript has no associated data or the data will not be deposited. [Authors' comment: The datasets used in this work to constrain the models are public data available in their respective references.]

Funded by SCOAP^3. SCOAP^3 supports the goals of the International Year of Basic Sciences for Sustainable Development.

Appendix A: Cosmological data sets and χ^2 measures

In this Appendix, we present some more details on the cosmological data sets and their χ^2 measures as used for the statistical analysis.

1. Cosmic microwave background (CMB)

The CMB data is given by the shift parameters which describe the location of the first peak in the temperature angular power spectrum. We use the shift parameters for Planck 2018 data [51], which includes temperature and polarization data, as well as CMB lensing, and given by the ratio between the model being tested and the LCDM model ($\mathbf{x}$ is a vector containing the model parameters) with a canonical cold dark matter as [82]

$$R(\mathbf{x}) = 100\sqrt{\Omega_m h^2}\,\frac{d_A^c(z_*,\mathbf{x})}{c},$$
$$\ell_a(\mathbf{x}) = \pi\,\frac{d_A^c(z_*,\mathbf{x})}{r_s(z_*,\mathbf{x})},$$

as well as $\Omega_b h^2$, with the reduced Hubble constant $h \equiv H_0/100\,\mathrm{km\,s^{-1}\,Mpc^{-1}}$. Here, $d_A^c(z_*,\mathbf{x})$ and $r_s(z_*,\mathbf{x})$ are the comoving angular-diameter distance and the sound horizon

$$d_A^c(z,\mathbf{x}) = \frac{c}{H_0}\frac{1}{\sqrt{\Omega_k}}\,\mathrm{Sinh}\left[\sqrt{\Omega_k}\int_0^z \frac{dz'}{E(z',\mathbf{x})}\right], \tag{A1}$$

$$r_s(z,\mathbf{x}) = \int_z^\infty \frac{c_s(z')dz'}{H(z',\mathbf{x})}, \tag{A2}$$

respectively, where $E(z,\mathbf{x}) \equiv H(z,\mathbf{x})/H_0$ and c_s is the sound speed

$$c_s(z) = \frac{c}{\sqrt{3[1+R_b(1+z)^{-1}]}} \tag{A3}$$

and

$$R_b = 31500\,\Omega_b h^2\,(T_{\mathrm{CMB}}/2.72)^{-4} \tag{A4}$$

at the photon-decoupling redshift z_*, given by [83]

$$z_* = 1048\left[1+0.00124\,(\Omega_b h^2)^{-0.738}\right]\left[1+g_1\,(\Omega_m h^2)^{g_2}\right],$$
$$g_1 = 0.0783\,(\Omega_b h^2)^{-0.238}\left[1+39.5\,(\Omega_b h^2)^{-0.763}\right]^{-1},$$
$$g_2 = 0.560\,\left[1+21.1\,(\Omega_b h^2)^{1.81}\right]^{-1}. \tag{A5}$$

Then, we obtain the χ^2 measure for Planck 2018 as

$$\chi^2_{\mathrm{Planck}} = (\Delta\mathcal{F}_{\mathrm{Planck}})^{\mathrm{T}}\,C^{-1}_{\mathrm{Planck}}\,\Delta\mathcal{F}_{\mathrm{Planck}}, \tag{A6}$$

where $\Delta\mathcal{F}_{\mathrm{Planck}} \equiv \mathcal{F}_{\mathrm{Planck(th)}} - \mathcal{F}_{\mathrm{Planck(obs)}}$ is the difference between the theoretical and observed distance modulus for a vector formed from the three shift parameters $\mathcal{F}_{\mathrm{Planck}} \equiv \{R, \ell_a, \Omega_b h^2\}$ and C^{-1}_{Planck} is the inverse covariance matrix [82].

2. Baryon acoustic oscillations (BAO)

The BAO consists of several data sets:

SDSS-BOSS This includes the data points from the Sloan Digital Sky Survey III – Baryon Acoustic Oscillation Spectroscopic Survey (SDSS-BOSS), DR12 release [52], with associated redshifts $z_B = \{0.38, 0.51, 0.61\}$. The pertinent quantities for the BOSS data are

$$d_A^c(z,\mathbf{x})\,\frac{r_s^{\mathrm{fid}}(z_d)}{r_s(z_d,\mathbf{x})},$$
$$H(z,\mathbf{x})\,\frac{r_s(z_d,\mathbf{x})}{r_s^{\mathrm{fid}}(z_d)} \tag{A7}$$

at the *dragging* redshift z_d which can be approximated as [84]

$$z_d = \frac{1291\,(\Omega_m h^2)^{0.251}}{1+0.659\,(\Omega_m h^2)^{0.828}}\left[1+b_1\,(\Omega_b h^2)^{b_2}\right],$$
$$b_1 = 0.313\,(\Omega_m h^2)^{-0.419}\left[1+0.607\,(\Omega_m h^2)^{0.6748}\right],$$
$$b_2 = 0.238\,(\Omega_m h^2)^{0.223}. \tag{A8}$$

Here, $r_s^{\rm fid}(z_d)$ is the same quantity evaluated for a fiducial/reference model and we take $r_s^{\rm fid}(z_d) = 147.78$ Mpc [52]. We then obtain its χ^2 measure as

$$\chi^2_{\rm BOSS} = (\Delta\mathcal{F}_{\rm BOSS})^{\rm T}\, C^{-1}_{\rm BOSS}\,\Delta\mathcal{F}_{\rm BOSS} \tag{A9}$$

with $\Delta\mathcal{F}_{\rm BOSS} \equiv \mathcal{F}_{\rm BOSS(th)} - \mathcal{F}_{\rm BOSS(obs)}$ for a vector $\mathcal{F}_{\rm BOSS} \equiv \left\{d_A^c(z_B) r_s^{\rm fid}(z_d)/r_s(z_d),\ H(z_B) r_s(z_d)/r_s^{\rm fid}(z_d)\right\}$ and $C^{-1}_{\rm BOSS}$ is the inverse covariance matrix found in [52].

SDSS-eBOSS There is one more data point in the extended Baryon Acoustic Oscillation Spectroscopic Survey (eBOSS) [53] at $z = 1.52$, which gives the value

$$D_V(1.52, \mathbf{x})\ \frac{r_s^{\rm fid}(z_d)}{r_s(z_d, \mathbf{x})} = 3843 \pm 147, \tag{A10}$$

where D_V is defined as

$$D_V(z, \mathbf{x}) = \left[d_A^c(z, \mathbf{x})^2 \frac{cz}{H(z, \mathbf{x})}\right]^{1/3}. \tag{A11}$$

We have then its χ^2 measure as

$$\chi^2_{\rm eBOSS} = \frac{\Delta\mathcal{F}_{\rm eBOSS}}{\sigma^2_{\rm eBOSS}} \tag{A12}$$

with $\Delta\mathcal{F}_{\rm eBOSS} \equiv \mathcal{F}_{\rm eBOSS(th)} - \mathcal{F}_{\rm eBOSS(obs)}$ for $\mathcal{F}_{\rm eBOSS} \equiv D_V(z = 1.52) r_s^{\rm fid}(z_d)/r_s(z_d)$ and the measurement error $\sigma_{\rm eBOSS}$.

SDSS-BOSS-Lyman-α The Quasar-Lyman-α forest from SDSS-III BOSS RD11 [54] gives the two data points as

$$d_A^c(z = 2.34, \mathbf{x})/r_s(z_d, \mathbf{x}) = 36.98^{+1.26}_{-1.18},$$
$$c/H(z = 2.34, \mathbf{x}) r_s(z = z_d, \mathbf{x}) = 9.00 \pm 0.22, \tag{A13}$$

and we obtain the corresponding χ^2 measure as

$$\chi^2_{\rm Lyman-\alpha} = \left(\Delta\mathcal{F}_{\rm Lyman-\alpha}\right)^{\rm T} C^{-1}_{\rm Lyman-\alpha}\,\Delta\mathcal{F}_{\rm Lyman-\alpha} \tag{A14}$$

with $\Delta\mathcal{F}_{\rm Lyman-\alpha} \equiv \mathcal{F}_{\rm Lyman-\alpha(th)} - \mathcal{F}_{\rm Lyman-\alpha(obs)}$ and $\mathcal{F}_{\rm Lyman-\alpha} \equiv \{d_A^c(z = 2.34)/r_s(z_d),\ c/H(z = 2.34) r_s(z_d)\}$.

WiggleZ This includes the data from the WiggleZ Dark Energy Survey at redshift points $z_{\rm W} = \{0.44, 0.6, 0.73\}$ [55]. Here, the pertinent quantities are the acoustic parameter

$$A(z, \mathbf{x}) = 100\sqrt{\Omega_m h^2}\ \frac{D_V(z, \mathbf{x})}{cz} \tag{A15}$$

and Alcock–Paczynski parameter

$$F(z, \mathbf{x}) = \frac{d_A^c(z, \mathbf{x}) H(z, \mathbf{x})}{c}, \tag{A16}$$

where D_V is defined as above (A11). We then obtain its χ^2 measure as

$$\chi^2_{\rm WiggleZ} = \left(\Delta\mathcal{F}_{\rm WiggleZ}\right)^{\rm T} C^{-1}_{\rm WiggleZ}\,\Delta\mathcal{F}_{\rm WiggleZ} \tag{A17}$$

with $\Delta\mathcal{F}_{\rm WiggleZ} \equiv \mathcal{F}_{\rm WiggleZ(th)} - \mathcal{F}_{\rm WiggleZ(obs)}$ and $\mathcal{F}_{\rm WiggleZ} \equiv \{A(z_W),\ F(z_W)\}$.

3. Type Ia supernovae (SNe Ia)

We use the recent Pantheon catalogue of Type Ia supernovae (SNe Ia) which consists of 1048 objects in the redshift range $0.01 < z < 2.26$ [56]. The data is expressed as the distance modulus

$$\mu(z, \mathbf{x}) = 5 \log d_L(z, \mathbf{x}) + \mu_0, \tag{A18}$$

where μ_0 is a nuisance parameter containing the supernova absolute magnitude and d_L is the luminosity distance

$$d_L(z, \mathbf{x}) \equiv (1+z) \cdot d_A^c(z, \mathbf{x}). \tag{A19}$$

Removing the nuisance parameter dependence via marginalizing over μ_0 [85], we obtain its χ^2 measure as

$$\chi^2_{\rm Pantheon} = a + \log\frac{e}{2\pi} - \frac{b^2}{e}, \tag{A20}$$

where $a \equiv \Delta\mu^{\rm T} C^{-1}_{\rm Pantheon}\Delta\mu$, $b \equiv \Delta\mu^{\rm T} C^{-1}_{\rm Pantheon} \cdot \mathbf{1}$, $c \equiv \mathbf{1}^{\rm T} \cdot C^{-1}_{\rm Pantheon} \cdot \mathbf{1}$ with $\Delta\mu = \mu_{\rm th} - \mu_{\rm obs}$ for each object and the inverse covariance matrix $C^{-1}_{\rm Pantheon}$ for the whole sample. Here, the theoretical value of the distance module (A18) is given by

$$\mu_{\rm th} = 5 \log\left[(1+z_{\rm hel}) \cdot d_A^c(z_{\rm cmb}, \mathbf{x})\right] + \mu_0, \tag{A21}$$

where $z_{\rm cmb}$ is the CMB restframe redshift and $z_{\rm hel}$ is the *heliocentric* redshifts which includes the effect of the peculiar velocity [86,87].

4. Gamma-ray bursts (GRBs)

We use the set of 79 Gamma-Ray Bursts (GRBs) in the range $1.44 < z < 8.1$, called the Mayflower sample [57], which was calibrated in a model independent manner. The pertinent quantity for GRBs is the distance modulus μ and therefore its χ^2 measure is in analogue with SNe Ia in the formula (A20). But the important difference is that there is no distinction between $z_{\rm cmb}$ and $z_{\rm hel}$ for the theoretical value of the distance module $\mu_{\rm th}$ in (A21).

5. Lensed quasars

We use the 6 lensed quasars from the recent release by the H0liCOW collaboration [58,88]. These quasars have multiple-lensed images from which a time delay due to the different light paths can be obtained. The time delay can be expressed as

$$t(\theta,\beta)=\frac{1+z_L}{c}\frac{D_L D_S}{D_{LS}}\left[\frac{1}{2}(\theta-\beta)^2-\psi(\theta)\right], \tag{A22}$$

where z_L is the lens redshift, ψ is the lensing potential, and θ, β are the angular position of the image and the source, respectively. The quantities D_L, D_S, and D_{LS} are the angular-diameter distances for lens $\rightarrow$ observer, source $\rightarrow$ observer, and source $\rightarrow$ lens, respectively, defined as

$$d_A(z,\mathbf{x})=\frac{d_A^c(z,\mathbf{x})}{1+z}, \tag{A23}$$

$$D_L=d_A(z_L,\mathbf{x}),\quad D_S=d_A(z_S,\mathbf{x}),$$

$$D_{LS}=\frac{1}{1+z_S}\left[(1+z_S)D_S-(1+z_L)D_L\right], \tag{A24}$$

where z_L is the source redshift. From the time-delay distance, the combination constrained by H0liCOW, defined as $D_{\Delta t}=(1+z_L)D_L D_S/D_{LS}$, we obtain its χ^2 measure as

$$\chi^2_{\rm H0liCOW}=\sum_{i=1}^{6}\frac{\left(D_{\Delta t,i}(\mathbf{x})-D^{\rm obs}_{\Delta t,i}\right)^2}{\sigma^2_{D_{\Delta t,i}}} \tag{A25}$$

with the observed values $D^{\rm obs}_{\Delta t,i}$ and the measurement errors $\sigma_{D_{\Delta t,i}}$.

6. Cosmic chronometers (CC)

We use the early elliptical and lenticular galaxies at different redshifts whose spectral properties can be traced with cosmic time t so that they can be used as *Cosmic Chronometers* (CC) by measuring the Hubble parameter $H(z)\equiv dz/dt(1+z)$, independently on cosmological models [89]. Then, using 25 measurements from the data set in the range $0.07<z<1.965$ [59],[18] we obtain its χ^2 measure as

$$\chi^2_{\rm CC}=\sum_{i=1}^{25}\frac{[H(z_i,\mathbf{x})-H_{\rm obs}(z_i)]^2}{\sigma^2_{\rm CC}(z_i)}, \tag{A26}$$

where $H_{\rm obs}(z_i)$ are the measured values of the Hubble parameter and $\sigma_{\rm CC}(z_i)$ are their measurement errors.

Appendix B: More details of constraints on parameters

See Figs. 4, 5, 6 and Table 2.

[18] In this paper, we have not used the latest data set in [90] (the range $0.3<z<0.5$), due to some uncertainty in the Hubble parameter from different stellar population models.

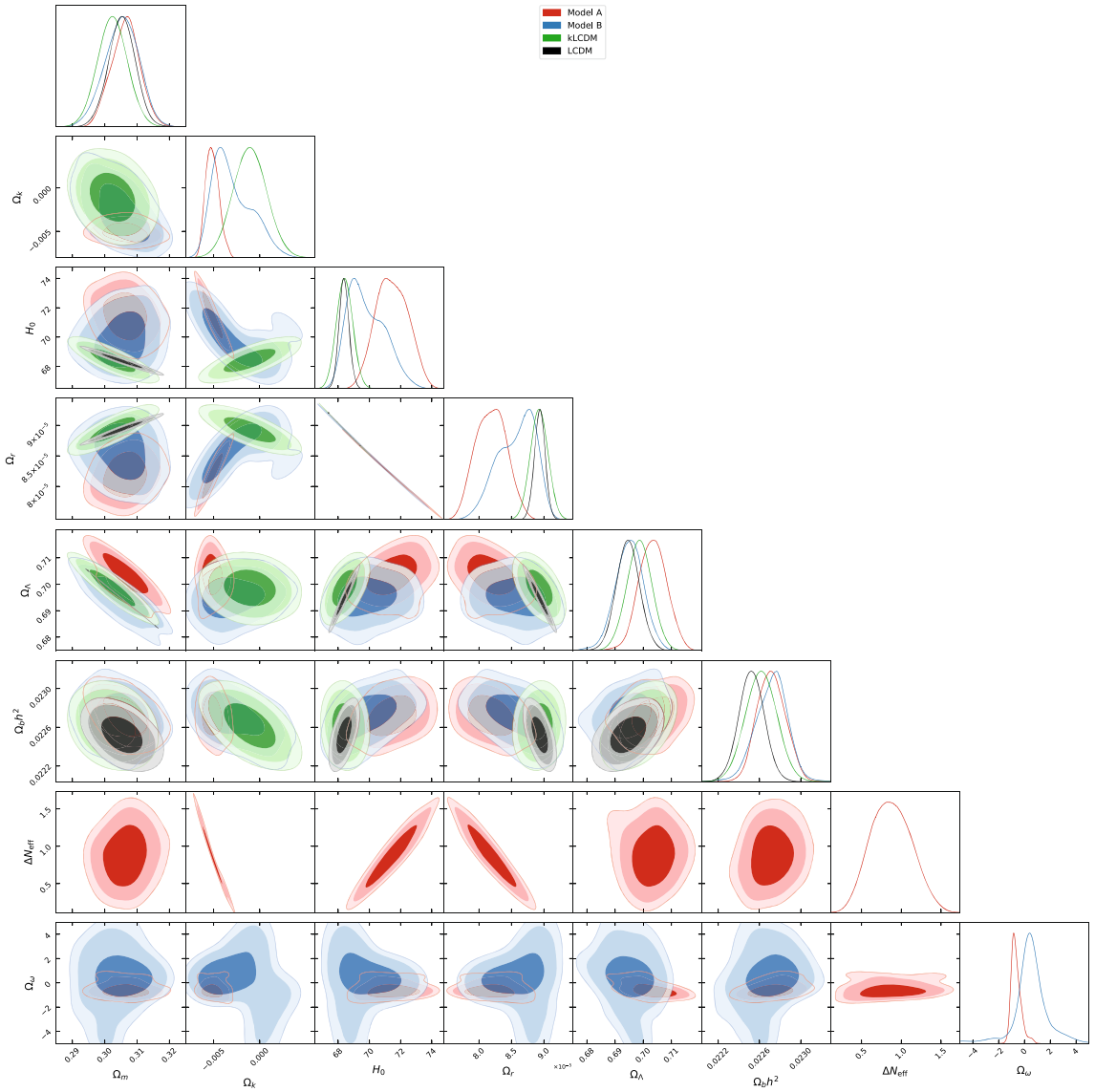

Fig. 4 2D joint and 1D marginalized posterior probability distributions for all the parameters in Table 1, obtained within the models **A**, **B**, LCDM, kLCDM. Contour plots are shown up to 3σ (99.7%) CL

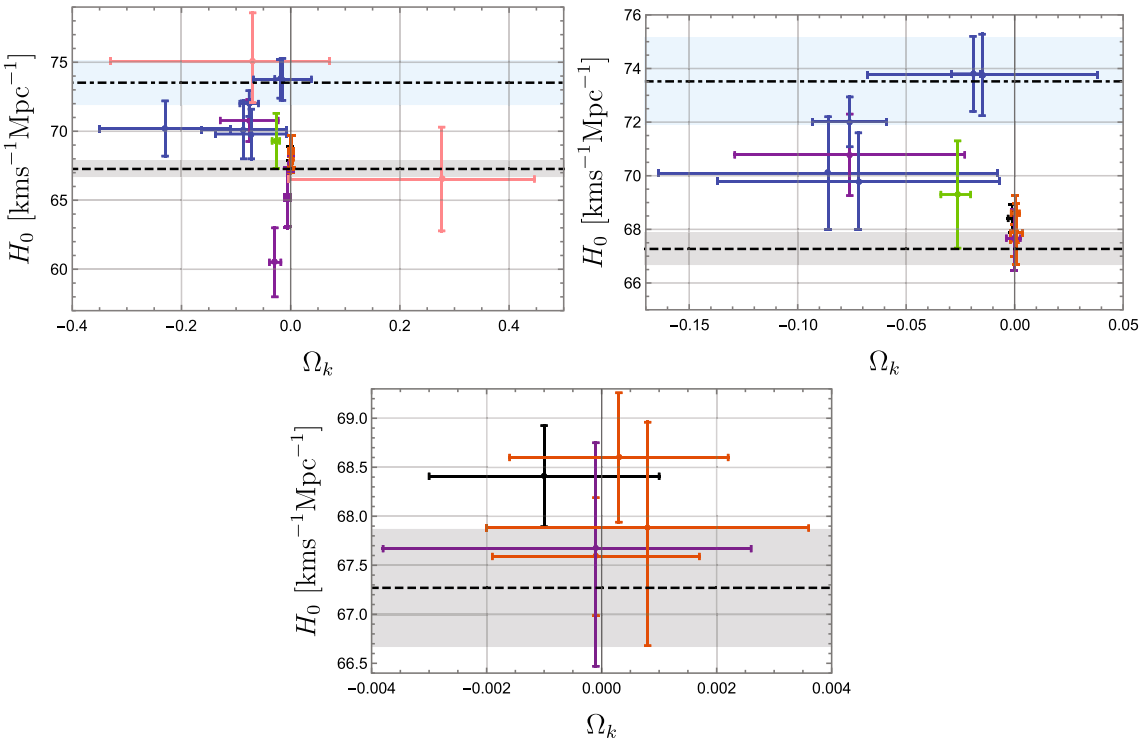

Fig. 5 Combined plots of the constraints on H_0 vs. Ω_k for the measurements in Fig. 2 and Fig. 3, based on (k)LCDM scenario. The companion data in Figs. 2 and 3 has the same color. The grey and blue vertical bands correspond the value of Planck 2018, $H_0 = 67.27 \pm 0.60$ km s^{-1} Mpc^{-1} [32], and the local measurement using Cepheids, $H_0 = 73.52 \pm 1.62$ km s^{-1} Mpc^{-1} [6], respectively, as in Figs. 2 and 3. By excluding some anomalous cases (top and rightmost oranges; leftmost blue; three purple data (bottom three)) with large errors in the full data (top left) and zooming the interested region (top right), one can see a *rough* tendency $H_0 \propto -|\Omega_k|$, as in the full contour plots in [28, Fig. 8] or [30, Fig. 3]. A few data points near $\Omega_k = 0$ do not show the tendency clearly but a further zooming (bottom) seems to show another tendency of the CMB+BAO cases in [30, Fig. 3]

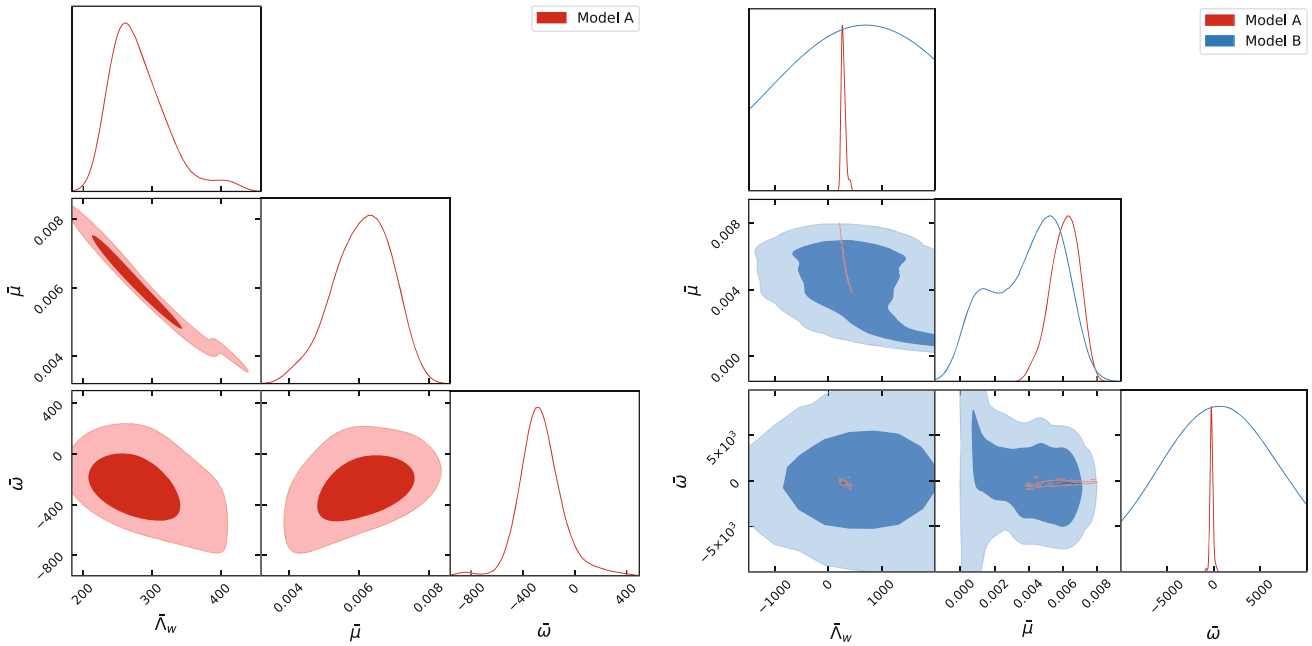

Fig. 6 2D joint and 1D marginalized posterior probability distributions for the theory parameters in Table 2, obtained within the models **A** (left), **B** (right), up to 2σ CL

Table 2 Constraints at 1σ CL on the theory parameters for our two cosmology models **A**, **B**

Theory parameters	Model **A**	Model **B**
$\bar{\omega}$	$-275.94^{+171.38}_{-133.08}$	$173.51^{+1357.96}_{-159.84}$
$\bar{\Lambda}_W$	$270.99^{+49.89}_{-31.65}$	$390.24^{+1224.34}_{-117.17}$
$\bar{\mu}$	$0.0062^{+0.0008}_{-0.0010}$	$0.0043^{+0.0018}_{-0.0033}$

References

1. A. Friedmann, Z. Phys. **10**, 377 (1922)
2. G. Lemaitre, Ann. Soc. Sci. Bruxelles A **47**, 49 (1927)
3. A.G. Riess et al. [Supernova Search Team], Astron. J. **116**, 1009 (1998). arXiv:astro-ph/9805201
4. E. Komatsu et al. [WMAP], Astrophys. J. Suppl. **192**, 18 (2011). arXiv:1001.4538 [astro-ph.CO]
5. A.G. Riess et al., Astrophys. J. **855**, 136 (2018). arXiv:1801.01120 [astro-ph.SR]
6. A.G. Riess et al., Astrophys. J. **876**, 85 (2019). arXiv:1903.07603 [astro-ph.CO]
7. M. Asgari et al., Astron. Astrophys. **634**, A127 (2020). arXiv:1910.05336 [astro-ph.CO]
8. E. Di Valentino et al., arXiv:2103.01183 [astro-ph.CO]
9. L. Perivolaropoulos, F. Skara, arXiv:2105.05208 [astro-ph.CO]
10. N. Schöneberg et al., arXiv:2107.10291 [astro-ph.CO]
11. K.S. Stelle, Phys. Rev. D **16**, 953 (1977)
12. E.M. Lifshitz, Zh. Eksp. Teor. Fiz. **11**, 255, 269 (1941)
13. B.S. DeWitt, Phys. Rev. **160**, 1113 (1967)
14. P. Hořava, Phys. Rev. D **79**, 084008 (2009). arXiv:0901.3775 [hep-th]
15. A. Wang, Int. J. Mod. Phys. D **26**, 1730014 (2017). arXiv:1701.06087 [gr-qc]
16. D.O. Devecioglu, M.I. Park, arXiv:2112.00576 [hep-th]
17. G.J. Olmo, D. Rubiera-Garcia, A. Wojnar, Phys. Rep. **876**, 1 (2020). arXiv:1912.05202 [gr-qc]
18. R. Abbott et al. [LIGO Scientific, VIRGO and KAGRA], arXiv:2112.06861 [gr-qc]
19. K. Kim et al., Phys. Rev. D **103**, 044052 (2021). arXiv:1810.07497 [gr-qc]
20. M. Liu et al., Gen. Relativ. Gravit. **43**, 1401 (2011). arXiv:1010.6149 [gr-qc]
21. G.P. Li, K.J. He, JCAP **06**, 037 (2021). arXiv:2105.08521 [gr-qc]
22. A. Emir Gümrükçüoğlu, M. Saravani, T.P. Sotiriou, Phys. Rev. D **97**, 024032 (2018). arXiv:1711.08845 [gr-qc]
23. Y. Gong et al., Phys. Rev. D **98**, 104017 (2018). arXiv:1808.00632 [gr-qc]
24. M. Khodadi, E.N. Saridakis, Phys. Dark Universe **32**, 100835 (2021). arXiv:2012.05186 [gr-qc]
25. T. Gupta et al., Class. Quantum Gravity **38**, 195003 (2021). arXiv:2104.04596 [gr-qc]
26. N. Frusciante et al., Phys. Dark Universe **13**, 7 (2016). arXiv:1508.01787 [astro-ph.CO]
27. N. Frusciante, M. Benetti, Phys. Rev. D **103**, 104060 (2021). arXiv:2005.14705 [astro-ph.CO]
28. E. Di Valentino, A. Melchiorri, J. Silk, Nat. Astron. **4**, 196 (2019). arXiv:1911.02087 [astro-ph.CO]
29. W. Handley, Phys. Rev. D **103**, L041301 (2021). arXiv:1908.09139 [astro-ph.CO]
30. E. Di Valentino, A. Melchiorri, J. Silk, Astrophys. J. Lett. **908**, L9 (2021). arXiv:2003.04935 [astro-ph.CO]
31. S. Alam et al. [eBOSS], Phys. Rev. D **103**, 083533 (2021). arXiv:2007.08991 [astro-ph.CO]
32. N. Aghanim et al. [Planck], Astron. Astrophys. **641**, A6 (2020). arXiv:1807.06209 [astro-ph.CO] [Erratum: Astron. Astrophys. **652**, C4 (2021)]
33. R.L. Arnowitt, S. Deser, C.W. Misner, Gen. Relativ. Gravit. **40**, 1997 (2008). arXiv:gr-qc/0405109
34. S. Mukohyama, JCAP **06**, 001 (2009). arXiv:0904.2190 [hep-th]
35. G. Geshnizjani, W.H. Kinney, A. Moradinezhad Dizgah, JCAP **11**, 049 (2011). arXiv:1107.1241 [astro-ph.CO]
36. S. Shin, M.I. Park, JCAP **12**, 033 (2017). arXiv:1701.03844 [hep-th]
37. M. Visser, arXiv:0912.4757 [hep-th]
38. D. Blas, O. Pujolas, S. Sibiryakov, Phys. Rev. Lett. **104**, 181302 (2010). arXiv:0909.3525 [hep-th]
39. D.O. Devecioglu, M.I. Park, Phys. Rev. D **99**, 104068 (2019). arXiv:1804.05698 [hep-th]
40. K. O'Neal-Ault, Q.G. Bailey, N.A. Nilsson, Phys. Rev. D **103**, 044010 (2021). arXiv:2009.00949 [gr-qc]
41. Y. Zhang et al., Mon. Not. R. Astron. Soc. **501**, 1013 (2021). arXiv:2007.12607 [astro-ph.CO]
42. M.I. Park, JHEP **09**, 123 (2009)
43. M.I. Park, JCAP **01**, 001 (2010). arXiv:0906.4275 [hep-th]
44. S. Dutta, E.N. Saridakis, JCAP **01**, 013 (2010). arXiv:0911.1435 [hep-th]
45. E.J. Son, W. Kim, JCAP **06**, 025 (2010). arXiv:1003.3055 [hep-th]
46. G. Steigman, Adv. High Energy Phys. **2012**, 268321 (2012). arXiv:1208.0032 [hep-ph]
47. N.A. Nilsson, E. Czuchry, Phys. Dark Universe **23**, 100253 (2019). arXiv:1803.03615 [gr-qc]
48. C.P. Robert, arXiv:1504.01896 [stat.CO]
49. J. Dunkley et al., Mon. Not. R. Astron. Soc. **356**, 925 (2005). arXiv:astro-ph/0405462 [astro-ph]
50. A. Lewis, arXiv:1910.13970 [astro-ph.IM]
51. Z. Zhai, Y. Wang, JCAP **07**, 005 (2019). arXiv:1811.07425 [astro-ph.CO]
52. S. Alam et al. [BOSS], Mon. Not. R. Astron. Soc. **470**, 2617 (2017). arXiv:1607.03155 [astro-ph.CO]
53. M. Ata et al., Mon. Not. R. Astron. Soc. **473**, 4773 (2018). arXiv:1705.06373 [astro-ph.CO]
54. V. de Sainte Agathe et al., Astron. Astrophys. **629**, A85 (2019). arXiv:1904.03400 [astro-ph.CO]
55. C. Blake et al., Mon. Not. R. Astron. Soc. **425**, 405 (2012). arXiv:1204.3674 [astro-ph.CO]
56. D.M. Scolnic et al., Astrophys. J. **859**, 101 (2018). arXiv:1710.00845 [astro-ph.CO]
57. J. Liu, H. Wei, Gen. Relativ. Gravit. **47**, 141 (2015). arXiv:1410.3960 [astro-ph.CO]
58. K.C. Wong et al., Mon. Not. R. Astron. Soc. **498**, 1420 (2020). arXiv:1907.04869 [astro-ph.CO]
59. M. Moresco, Mon. Not. R. Astron. Soc. **450**, L16 (2015). arXiv:1503.01116 [astro-ph.CO]
60. G. Efstathiou, S. Gratton, Mon. Not. R. Astron. Soc. **496**, L91 (2020). arXiv:2002.06892 [astro-ph.CO]
61. J.E. Gonzalez et al., JCAP **11**, 060 (2021). arXiv:2104.13455 [astro-ph.CO]
62. C.G. Park, B. Ratra, Astrophys. Space Sci. **364**, 134 (2019). arXiv:1809.03598 [astro-ph.CO]
63. R.C. Nunes, A. Bernui, Eur. Phys. J. C **80**, 1025 (2020). arXiv:2008.03259 [astro-ph.CO]
64. D. Benisty, D. Staicova, Astron. Astrophys. **647**, A38 (2021). arXiv:2009.10701 [astro-ph.CO]
65. S. Vagnozzi et al., Phys. Dark Universe **33**, 100851 (2021). arXiv:2010.02230 [astro-ph.CO]
66. S. Vagnozzi, A. Loeb, M. Moresco, Astrophys. J. **908**, 84 (2021). arXiv:2011.11645 [astro-ph.CO]
67. https://wiki.cosmos.esa.int/planck-legacy-archive/images/2/21/Baseline_params_table_2018_95pc_v2.pdf

68. Z. Zhai et al., JCAP **07**, 009 (2020). arXiv:1912.04921 [astro-ph.CO]
69. L. Balkenhol et al. [SPT-3G], Phys. Rev. D **104**, 083509 (2021). arXiv:2103.13618 [astro-ph.CO]
70. G. Mangano, G. Miele, S. Pastor, M. Peloso, Phys. Lett. B **534**, 8 (2002). arXiv:astro-ph/0111408
71. M.M. Flores, A. Kusenko, Phys. Rev. Lett. **126**, 041101 (2021). arXiv:2008.12456 [astro-ph.CO]
72. L.L. Graef, M. Benetti, J.S. Alcaniz, Phys. Rev. D **99**, 043519 (2019). arXiv:1809.04501 [astro-ph.CO]
73. H. Jeffreys, *The Theory of Probability* (Oxford University Press, Oxford, 1961)
74. R.E. Kass, A.E. Raftery, J. Am. Stat. Assoc. **90**, 773 (1995)
75. S. Nesseris, J. Garcia-Bellido, JCAP **08**, 036 (2013). arXiv:1210.7652 [astro-ph.CO]
76. R. Trotta, Contemp. Phys. **49**, 71 (2008). arXiv:0803.4089 [astro-ph]
77. C. Argüelles, N. Grandi, M.I. Park, JHEP **10**, 100 (2015). arXiv:1508.04380 [hep-th]
78. L. Knox, M. Millea, Phys. Rev. D **101**, 043533 (2020). arXiv:1908.03663 [astro-ph.CO]
79. A.G. Riess et al., Astrophys. J. Lett. **908**, L6 (2021). arXiv:2012.08534 [astro-ph.CO]
80. A. Lewis, A. Challinor, A. Lasenby, Astrophys. J. **538**, 473 (2000). arXiv:astro-ph/9911177 [astro-ph]
81. J. Lesgourgues, arXiv:1104.2932 [astro-ph.IM]
82. Y. Wang, M. Dai, Phys. Rev. D **94**, 083521 (2016). arXiv:1509.02198 [astro-ph.CO]
83. W. Hu, N. Sugiyama, Astrophys. J. **471**, 542–570 (1996). arXiv:astro-ph/9510117
84. D.J. Eisenstein, W. Hu, Astrophys. J. **496**, 605 (1998). arXiv:astro-ph/9709112
85. A. Conley et al. [SNLS], Astrophys. J. Suppl. **192**, 1 (2011). arXiv:1104.1443 [astro-ph.CO]
86. L. Hui, P.B. Greene, Phys. Rev. D **73**, 123526 (2006). arXiv:astro-ph/0512159
87. Y. Wang, S. Wang, Phys. Rev. D **88**, 043522 (2013). arXiv:1304.4514 [astro-ph.CO] [Erratum: Phys. Rev. D **88**, 069903 (2013)]
88. S.H. Suyu et al., Mon. Not. R. Astron. Soc. **468**, 2590 (2017). arXiv:1607.00017 [astro-ph.CO]
89. R. Jimenez, A. Loeb, Astrophys. J. **573**, 37 (2002). arXiv:astro-ph/0106145
90. M. Moresco et al., JCAP **05**, 014 (2016). arXiv:1601.01701 [astro-ph.CO]